

Reduction Photolithography Using Microlens Arrays: Applications in Gray Scale Photolithography

Hongkai Wu,[†] Teri W. Odom,[†] and George M. Whitesides*

Department of Chemistry and Chemical Biology, Harvard University, 12 Oxford Street, Cambridge, Massachusetts 02138

This paper describes the application of reduction photolithography, using arrays of microlenses and gray scale masks, to generate arrays of micropatterns having multilevel and curved features in photoresist. This technique can fabricate, in a single exposure, three-dimensional microstructures (e.g., nonspherical microlens arrays) over areas of $\sim 2 \times 2$ cm². The simple optical configuration consisted of transparency film (having centimeter-sized features) as gray scale photomasks, an overhead projector as the illumination source, and arrays of microlenses as the size-reducing elements. Arrays of 40- and 100- μ m lenses achieved a lateral size reduction of $\sim 10^3$ and generated patterns of well-defined, multilevel structures; these structures may find use in applications such as diffractive optics.

This paper describes the combined use of arrays of microlenses and gray scale photolithography to fabricate arrays of multilevel structures in photoresist in a single exposure. Microlens arrays are widely used as beam collimators, light collectors, and fiber-optic couplers or connectors,^{1–5} and arrays of stacked columns of microlenses have recently been used to replicate patterns from photomasks into photoresist.⁶ We have begun to develop arrays of microlenses for use in microfabrication of simple, repetitive patterns.^{7–9} Appropriate microlens arrays, used in reduction photolithography, enable size reductions of $\sim 10^3$ and patterning of areas over several square centimeters in a single exposure step. These exposures through the lens arrays transfer a macroscopic figure on the photomask into micropatterns in photoresist on a planar substrate. This method can generate many kinds of arrays of micropatterns that can have (1) various lattice

symmetries, all easily determined by the symmetry of the lens array; (2) various kinds of structures, determined by the figure on the mask; and (3) various sizes, tuned by changing the optical properties of the lenses.

Three-dimensional (3D) microstructures having well-defined features in periodic arrays are important as optical elements (e.g., microlens arrays, diffractive optical elements, and gratings). Several techniques can generate 3D microstructures in photoresist;^{5,10,11} two serial methods include (1) direct laser writing¹² and (2) photolithography using binary masks, followed by reactive ion etching (RIE).^{13–15} The direct laser writing technique is straightforward—different doses of laser light generate features having different heights—but this method requires careful control of etching and baking conditions. The iterative process using binary masks, involving n repetitions of photolithography, RIE, and precision alignment, can generate n -level structures that act as analogues of continuous, 3D structures. Major drawbacks to these methods include the cost and complexity of the equipment required and the amount of time (due to serial writing and multiple exposure steps) necessary to form arrays of structures.

An alternative route to multilevel structures is gray scale lithography.¹⁶ This photolithographic technique can create high-quality, multilevel optical elements having both sharp and curved features in a single exposure without the need for multiple alignment steps. The key to this technique is the use of gray scale photomasks, which modulate the light intensity according to their levels of gray. Two types of masks commonly used in gray scale lithography include halftone chrome masks^{17–19} and high-energy-beam-sensitive (HEBS) glass masks.^{20,21} Halftone masks are

* Corresponding author. Phone: (617) 495-9430. Fax: (617) 495-9857. E-mail: gwhitesides@gmwhgroup.harvard.edu.

[†] These authors contributed equally to this work.

- (1) Daly, D. *Microlens Arrays*; Taylor & Francis: New York, 2000.
- (2) Hutley, M.; Stevens, R.; Daly, D. *Phys. World* **1991**, 4, 27–32.
- (3) <http://www.memsoptical.com>.
- (4) Rabarot, M.; Fulbert, L.; Molva, E.; Thony, P.; Marty, V.; Dastouet, S. *Pure Appl. Opt.* **1997**, 6, 6699–705.
- (5) Sankur, H. O.; Motamedi, M. E. *Proc. SPIE-Int. Soc. Opt. Eng.* **2000**, 4179, 30–55 (*Micromachining Technology for Micro-Optics*).
- (6) Völkel, R.; Herzig, H. P.; Ph., N.; Dändliker, R. *Opt. Eng.* **1996**, 35, 3323–3330.
- (7) Wu, M. H.; Whitesides, G. M. *Appl. Phys. Lett.* **2001**, 78, 2273–2275.
- (8) Wu, M. H.; Whitesides, G. M. *Langmuir*. Submitted.
- (9) Wu, M. H.; Paul, K. E.; Yang, J.; Whitesides, G. M. *Appl. Phys. Lett.* **2002**, 80, 3500–3502.

- (10) Schilling, A.; Nussbaum, P.; Philipoussis, I.; Herzig, H. P.; Stauffer, L.; Rossi, M.; Kley, E. B. *Proc. SPIE-Int. Soc. Opt. Eng.* **2000**, 4179, 65–72 (*Micromachining Technology for Micro-Optics*).
- (11) Suleski, T. J.; Baggett, B.; Delaney, W. F.; Kathman, A. D. *Proc. SPIE-Int. Soc. Opt. Eng.* **1999**, 3633, 26–34 (*Diffractive and Holographic Technologies, Systems, and Spatial Light Modulators VI*).
- (12) Gale, M. T.; Rossi, M.; Pedersen, J.; Schuetz, H. *Opt. Eng.* **1994**, 33, 3556–3566.
- (13) Brown, D. M.; Brown, D. R.; Brown, J. D. *Proc. SPIE-Int. Soc. Opt. Eng.* **1999**, 3633, 46–50 (*Diffractive and Holographic Technologies, Systems, and Spatial Light Modulators VI*).
- (14) Kudryachov, V. A.; Lee, S. *Microelectron. Eng.* **2001**, 57–58, 819–823.
- (15) David, C. *Microelectron. Eng.* **2000**, 53, 677–680.
- (16) Kley, E. B. *Microelectron. Eng.* **1997**, 34, 261–298.
- (17) Quentel, F.; Fieret, J.; Holmes, A. S.; Paineau, S. *Proc. SPIE-Int. Soc. Opt. Eng.* **2001**, 4274, 420–431 (*Laser Applications in Microelectronic and Optoelectronic Manufacturing VI*).
- (18) Navarrete-Garcia, E.; Calixto, S. *Proc. SPIE-Int. Soc. Opt. Eng.* **1998**, 3511, 385–392 (*Micromachining and Microfabrication Process Technology IV*).

essentially binary chrome masks that are designed in CAD drawing programs; the gray levels in these masks are simulated by different densities of opaque pixels on a transparent background. HEBS glass masks are fabricated by exposing this glass to controlled doses of a high-energy electron beam; this exposure causes the reduction of silver ions in the glass. Areas of the mask with high concentrations of reduced silver ions correspond to high levels of gray shading. These methods that use gray scale masks to fabricate multilevel structures transfer the patterns on the masks into photoresist without any size reduction. The generation of 3D structures having micrometer-sized features requires careful construction of the sharp gradient of gray levels in the micrometer scale on the mask.

We have developed a simple technique to generate micropatterns of multilevel structures using microlens arrays with gray scale masks made from transparency films. Microlens arrays reduce the macroscopic figures on the photomasks into arrays of micropatterns; the gray levels on the masks modulate the intensity of the illumination through each lens and this modulation results in features having variations in height. This procedure required a minimal optical setup: an overhead projector equipped with a halogen bulb as the broadband illumination source, transparency films as gray scale photomasks, and arrays of microlenses as the size-reduction elements. Using arrays of 40- and 100- μm lenses, we were able to achieve a size reduction of $\sim 10^3$ over areas of $\sim 2 \times 2 \text{ cm}^2$ and to generate micropatterns having well-defined, multilevel features in photoresist. We believe that such structures will be useful as optical elements, 3D structures for cell culture, arrays of microreactors, and microfluidic systems.

EXPERIMENTAL DESIGN

Fabrication of Microlens Arrays. Many methods have been developed to fabricate arrays of microlenses. These methods include the assembly of microspheres into close-packed monolayers,⁷ dip-coating (and then curing) liquid polymers on patterned, self-assembled monolayers of alkanethiols,²² melting colloids of polymers in a template of patterned holes in photoresist (followed by removal of the photoresist),²³ and melting posts of photoresist patterned on transparent substrates.^{2,24} We prepared our microlens arrays by the melting technique, with one adaptation: an opaque layer was added between adjacent microlenses to prevent light from the illumination source from passing between the lenses.

Figure 1A summarizes the procedure we used to fabricate the microlens arrays. First, we spin-coated a layer of positive photoresist (Shipley 1818, index of refraction $n_{\text{lens}} = 1.59$) onto a glass slide coated with a thin (10-nm) layer of gold and patterned the photoresist into an array of circular posts (40 or 100 μm in diameter) through a chrome mask. This layer of gold was transparent to the wavelengths in the visible regime (absorbance $\sim 0.2\text{--}0.3$). Second, we heated and melted the photoresist posts

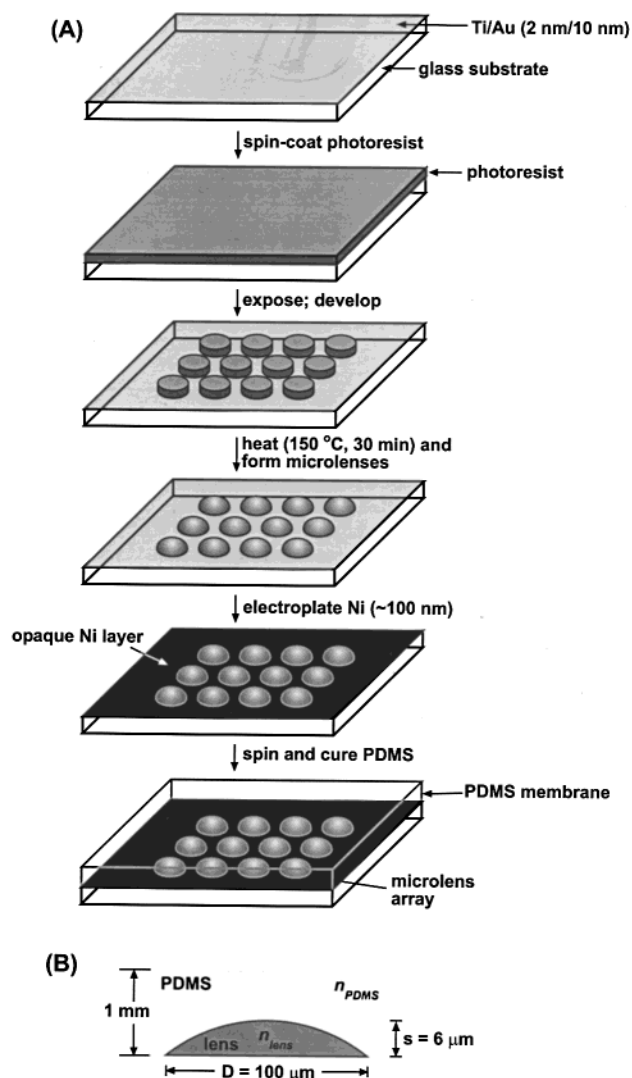


Figure 1. (A) Schematic procedure to fabricate a microlens array assembly. The characteristics of the arrays of lenses—the diameter of the lenses and their positions in the arrays—are determined by photolithography. The curvature and focal length of the lenses is determined by the diameter of the circular post and the thickness of the photoresist layer. (B) Schematic diagram of a cross section of a 100- μm lens in the microlens array used in our experiments and its dimensions.

($T_g \sim 100 \text{ }^\circ\text{C}$) on a hot plate at 150 $^\circ\text{C}$ for 30 min to form microlenses.²⁵ The posts of photoresist minimized their surface energies by reflowing to form a section of a sphere. The optical properties (e.g., focal length) of the microlenses were determined by the thickness of the photoresist and the size of the circular patterns (either 40 or 100 μm) on the chrome mask. Third, we electroplated an opaque layer ($\sim 100 \text{ nm}$) of nickel onto the areas of gold not covered by microlenses; this layer allowed exposure of photoresist only by light that had been focused by the lenses. This blocking layer was important to establish a relationship between the exposure time and the depth of the photoresist after development. Finally, we spin-coated a layer of poly(dimethylsiloxane) (PDMS) (index of refraction $n_{\text{PDMS}} = 1.4$) onto the array of microlenses. This layer of PDMS, whose thickness was

(19) Henke, W.; Hoppe, W.; Quenzer, H. J.; Staudt-Fischbach, P.; Wagner, B. *Microelectron. Eng.* **1995**, *27*, 267–270.
 (20) Long, P.; Daschner, W.; Johnson, E.; Lee, S. H. *Proc. SPIE-Int. Soc. Opt. Eng.* **1997**, *3010*, 105–110 (*Diffraction and Holographic Device Technologies and Applications IV*).
 (21) Daschner, W.; Long, P.; Stein, R.; Wu, C.; Lee, S. H. *J. Vac. Sci. Technol.*, **1996**, *14*, 3730–3733.
 (22) Biebuyck, H. A.; Whitesides, G. M. *Langmuir* **1994**, *10*, 2790–2793.
 (23) Lu, Y.; Yin, Y.; Xia, Y. *Adv. Mater.* **2001**, *13*, 34–37.
 (24) Popovic, Z. D.; Sprague, R. A.; Neville-Connell, G. A. *Appl. Opt.* **1988**, *27*, 1281–1284.

(25) During the heating process, the liquefied photoresist spread slightly ($< 5\%$) on the substrates.

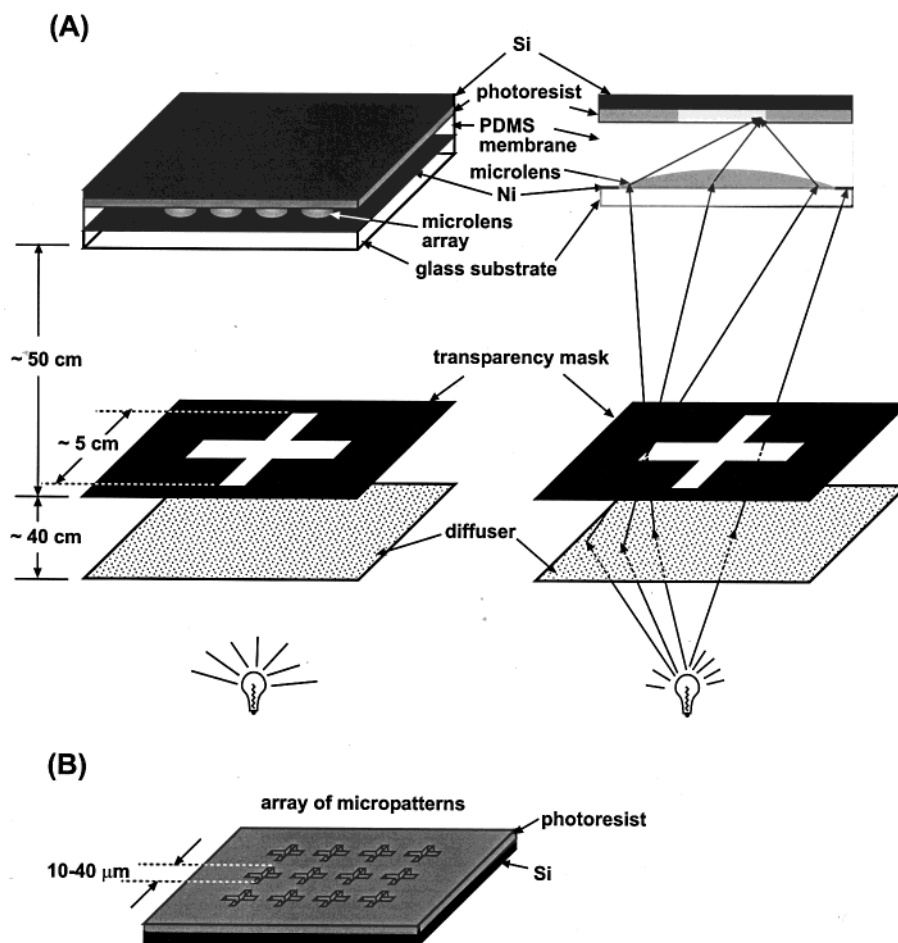


Figure 2. (A) Left: scheme of reduction lithography using microlens arrays. Right: Schematic illustration of the path of the light from the lamp, through the diffuser and photomask, to the lenses. Each lens reduces and focuses the figure on the mask into the photoresist. (B) After exposure and development, an array of pattern with the same figure as in the photomask was formed in the photoresist.

controlled to be equal to the calculated focal length of the lenses, was a convenient way to situate the photoresist-coated substrate in the image plane of the microlenses.

Calculation of the Focal Length of the Microlenses. The focal length f of the lenses depends on n_{lens} , n_{PDMS} , the diameter D of the base of the lens, and the thickness s of the lens (Figure 1B). The thickness of the lenses was measured using atomic force microscopy (AFM). From simple geometrical optics,³ the focal length of a thin, plano-convex lens is given by eq 1. For $n_{\text{lens}} =$

$$f = ((D/2)^2 + s^2) / 2s(n_{\text{lens}} - n_{\text{PDMS}}) \quad (1)$$

1.59, $n_{\text{PDMS}} = 1.4$, $D = 100 \mu\text{m}$, and $s \sim 6 \mu\text{m}$, the focal length is $\sim 1 \text{ mm}$.

Configuration of the Optical System. Figure 2A shows a schematic diagram of the optical system used in reduction photolithography using microlens arrays. The microlens arrays were situated on a vertical stage at a distance of $\sim 50 \text{ cm}$ above the photomask and overhead projector, which we used as our broadband light source ($\sim 450\text{--}1200 \text{ nm}$). This distance is the maximum allowable for this projector setup and was chosen to produce large areas of uniform patterning ($2 \times 2 \text{ cm}^2$) and to generate the maximum size reduction of the mask.

We designed photomasks having various shapes and levels of gray with CAD software (Macromedia Freehand 10) and printed

them on transparency films with a desktop printer. Each mask had features covering a square area ($2 \times 2 \text{ in.}^2$) and was placed in the center of the projector. A ground glass diffuser (1.6 mm thick) was placed in front of the halogen bulb in order to randomize the direction of the light. After passing through the transparent regions of the photomask, the diffused light was focused by each microlens. Typical exposure times were between 20 and 90 s, and the development times were around 2 min. After development, each microlens formed an image of the mask in the photoresist (Figure 2B).

RESULTS AND DISCUSSION

Microlens Array Reduction Photolithography. Figure 3A shows an optical image of an array of $40\text{-}\mu\text{m}$ microlenses; each microlens is $\sim 4 \mu\text{m}$ thick with a focal length $\sim 275 \mu\text{m}$. Transparency masks having a single cross were used to generate micropatterns of crosses in photoresist; we transferred these patterns into chromium by liftoff, using e-beam evaporation to deposit 30 nm of chromium (Figure 3B). These patterns retained the same symmetry as the array of microlenses (square lattice with spacing of $100 \mu\text{m}$), and each image had a lateral size reduction of $\sim 10^3$. To resolve the minimum critical dimension of the images generated by these $40\text{-}\mu\text{m}$ lenses, we designed a series of photomasks having a single cross with minimum dimensions ranging from 5 mm to $100 \mu\text{m}$. Masks with line widths that were 5 mm generated

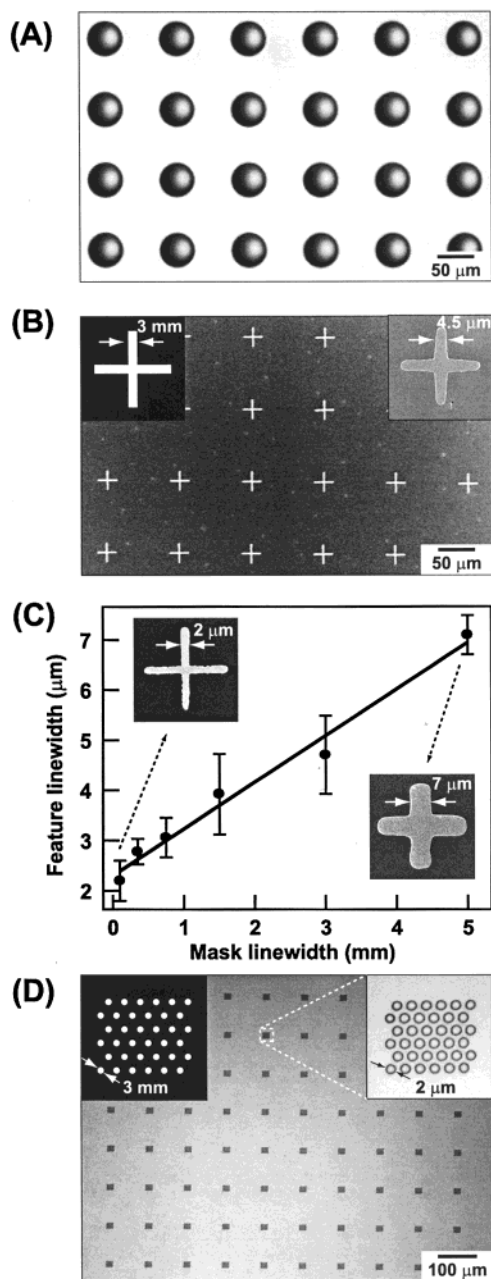


Figure 3. (A) Optical micrograph of the microlens array used in these experiments. (B) SEM image of a typical pattern formed by reduction lithography with the lens array shown in (A). These patterns are Cr (white crosses) on Si (dark region). The left top inset shows the photomask used for these exposures and the right top inset is a zoom-in SEM image showing a single cross. (C) Plot of line width of the crosses in photomasks versus line width of each cross in the images. A straight line is fit and drawn through the points. (D) Optical image of a uniform array of circles in photoresist formed with a hexagonal array of 36 circles in the mask. The left top inset shows the photomask used for these exposures and the right top inset shows a zoom-in optical image of the circle array generated by a single lens.

features in photoresist whose smallest size was $7.1 \pm 0.4 \mu\text{m}$, and masks with line widths that were $100 \mu\text{m}$ generated features whose smallest size was $2.1 \pm 0.2 \mu\text{m}$. Figure 3C shows how the dimensions of the images vary with the dimensions of the mask; the solid line is a linear fit to the data. The largest reduction achieved by this microlens arrays is ~ 700 times. It is possible to obtain narrower line widths by either increasing the thickness of

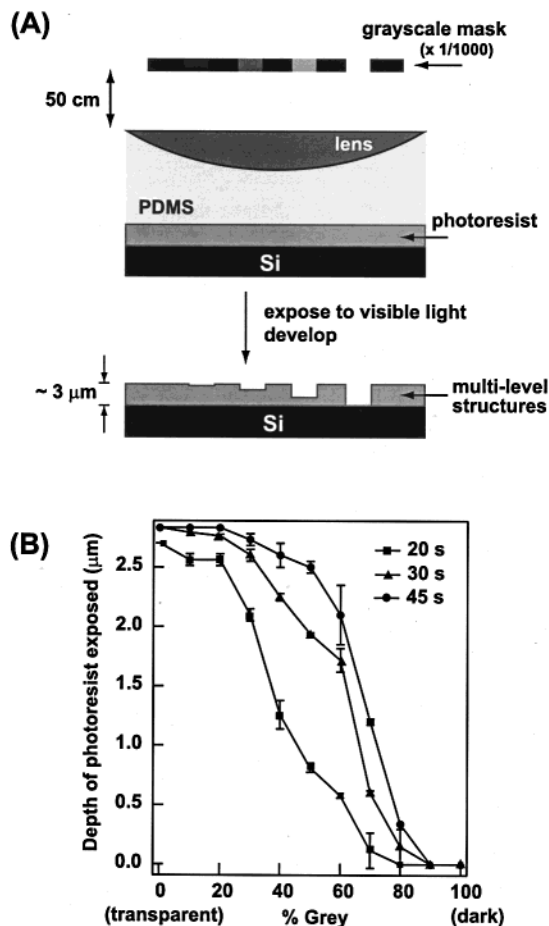


Figure 4. (A) Scheme to generate multilevel structures with a gray scale mask in microlens reduction lithography using a single exposure. The darker regions of the mask block more light than lighter regions, and thus the photoresist directly underneath these darker regions is exposed to a higher dose of light. (B) Plot of depth of developed photoresist versus the gray shading of the photomask. Three different exposure times (20, 30, 45 s) were explored. The development time was fixed at 2 min. The depth of the photoresist was measured by AFM and averaged from different areas for each sample.

the lens (which reduces the focal length) or decreasing the diameter of the lens (which limits the overall size of the image).

More complex patterns can be generated in photoresist by changing the figures on the photomasks. Figure 3D shows an example of how arrays of arrays can be formed: a hexagonal array of circles (each reduced uniformly from 3 mm in the mask to 2 μm in photoresist) is arranged in the square lattice symmetry of the lens array.

These micropatterns in photoresist did not exhibit distortions over an area of $2 \times 2 \text{ cm}^2$ in the area directly above the light source. This area of micrometer-sized features is comparable to those that are generated using commercial chrome masks in contact lithography. Distortions in the images in outer regions ($>1^\circ$ solid angle) are determined by (1) the position of the lens relative to the center of the mask and (2) the size and shape of the figure on the mask.

Gray Scale Photolithography. The demonstrations discussed to this point used binary photomasks of transparency film, that is, masks that only included transparent (0% gray) and black (100% gray) regions. Binary masks (with a single exposure) can only

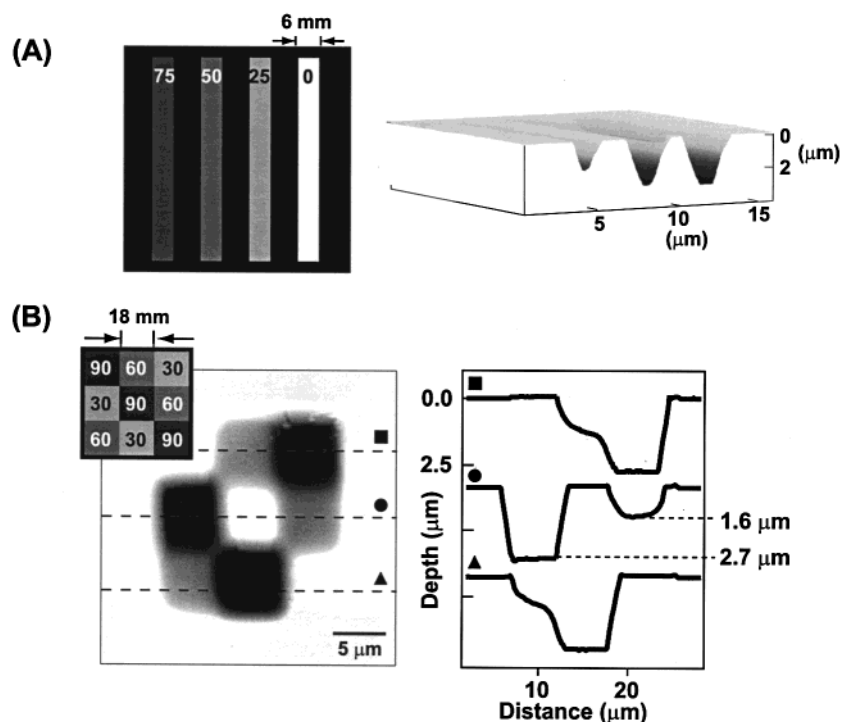


Figure 5. Generation of complex, multilevel structures with gray scale masks using microlens reduction photolithography with the 40- μm lenses. (A) 3D AFM image of lines having different gray levels (25, 50, 75%) interspersed with 100% gray levels. (B) AFM image of a checkerboard structure in photoresist generated from a mask of a checkerboard pattern with three levels of gray (30, 60, 90%) against a black background. Inset shows the pattern of the photomask. Profiles of several sections are shown on the right.

generate two-dimensional structures. Gray scale masks—the addition of gray levels, or different densities of black pixels, to the transparent regions of the photomasks—can generate 3D structures in a single exposure. For positive-tone photoresist, large exposure doses (corresponding to low gray levels in the photomask) result in deep features in the photoresist after development (Figure 4A).

Establishing the Relationship between Gray Level and Photoresist Depth. We designed a series of large-scale masks ($2 \times 2 \text{ in.}^2$) with uniform gray scale shading (0–100%, in increments of 10%) to quantify the levels of gray in the transparency mask with photoresist (Shipley 1818) depth after development. Figure 4B shows that the depth of the photoresist decreased nonlinearly with increased gray levels. We investigated these trends as a function of exposure time—20, 30, and 45 s—with a fixed development time of 2 min. All exposures resulted in a sharp drop in depth of photoresist at intermediate levels of gray (30–70%). For short exposure times (20 s or less), the intermediate region exhibited a near-linear relationship between photoresist depth and gray levels; longer exposure times showed a nonlinear relationship.

Generation of Three-Dimensional Structures. Using the gray scale plot in Figure 4B, we designed photomasks with varying levels of gray to generate different kinds of 3D structures in photoresist. We produced two classes of structures: (1) features with stepped profiles and (2) features with curved and linear profiles. The procedures we used were not optimized, and we made no effort to account for diffraction, off-axis illumination, or other relevant optical effects. These studies were intended to prototype a process for generating 3D profiles in photoresist.

Structures with Stepped Profiles. Figure 5A shows structures in photoresist formed from photomasks having strips of different levels of gray (75, 50, 25, 0%) separated by regions of black (100% gray). The depths of these trenches for the different gray levels corresponded well with the gray scale curve for an exposure time of 30 s. Figure 5B shows the result of photolithography using a gray scale mask where different levels of gray (30, 60, 90%) are adjacent to each other in a checkerboard pattern. The depths of these features are also in good agreement with those from the gray scale curve for the same exposure times (30 s)—1.6 μm at 60% gray and 2.7 μm at 30% gray. The variations in size among squares produced by different levels of gray, and the blurring of edges between them, were probably caused in part by diffraction of the incident light at the edges of each square of the mask.

Structures with Curved and Linear Profiles. We generated structures with curved and sloped profiles by using photomasks having a gradient of gray levels and by exposing for different amounts of time. Panels A and B of Figure 6 demonstrate how convex and concave lenses can be formed from gray scale masks having (1) a circular shape and (2) a gray scale gradient that extended radially from the center to the edge of the mask. The curved profiles of the lenses were generated by designing photomasks to have a gradient that varied linearly from 30 to 70% for the concave lenses and from 70 to 30% for the convex lenses. Long exposure times (45 s) were used to generate these curved profiles. We used short exposure times with the same continuous gradient (30–70%) to generate linear profiles. Figure 6C shows an example of the height profile of a structure generated in photoresist after short exposure times (20 s).

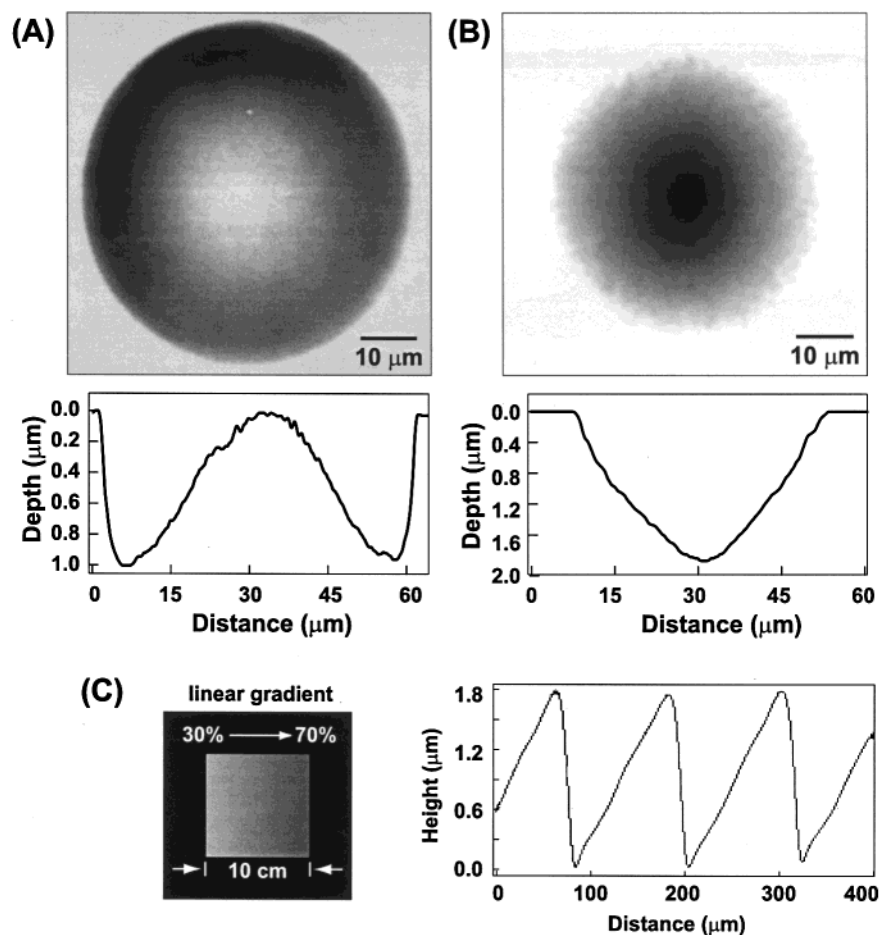


Figure 6. Generation of 3D structures in photoresist using 100- μm lenses. (A) AFM image of a convex microlens formed from a black-background transparency mask with a single circle (5 cm in diameter) having a radial gradient from 70% gray (center of mask) to 30% gray (edge of mask). (B) AFM image of a concave microlens formed from a black-background transparency mask with a single circle (5 cm in diameter) having a radial gradient from 30% gray (center of mask) to 70% gray (edge of mask). (C) Left: mask with a square area ($10 \times 10 \text{ cm}^2$) having a continuous, linear gradient from 30 to 70% gray. Right: height profile of a multilevel structure formed in photoresist using the mask on the left. The linear slopes were achieved by using the linear region of the gray scale characterization plot (30–70% gray) at short exposure times (20 s).

CONCLUSIONS

We have demonstrated that reduction photolithography using microlens arrays and gray scale transparency masks can combine to generate 3D microstructures with features sizes down to 2 μm over large areas ($2 \times 2 \text{ cm}^2$). Key advantages of this strategy include the following: (1) cost-effective equipment—no cleanroom, UV source, or collimation of light is required; and (2) transparency films as gray scale masks—easy and fast to generate (hours vs weeks for other techniques) and inexpensive compared to other gray scale masks (\$20 vs >\$500); (3) flexibility of microlenses—one set of lenses can generate many different patterns. Disadvantages of this technique include the following: (1) distortions in outer regions of the photoresist-coated substrate; (2) diffraction at the edges of the features in the mask; and (3) limited depth of focus of the lenses (estimated to be $\sim 5\text{--}10 \mu\text{m}$ for the microlenses in these experiments) constraining the range of microstructures that can be generated.

EXPERIMENTAL SECTION

Materials. Ti (99.99+%), Au (99.99+%), acetone, methanol, and hexamethyldisilazane (HMDS) were bought from Aldrich and

used as received. Microposit 1805 and 1818 photoresist (Shipley Co. Inc., Marlborough, MA) and Microposit 351 developer (Shipley Co. Inc.) were used as received. Poly(dimethylsiloxane) (Sylgard 184) was ordered from Dow Corning, Midland, MI; the two components (prepolymer and the catalyst) were mixed thoroughly by mass ratio 10:1 and degassed for 1 h before use.

Fabrication of Microlens Array. Glass slides were sonicated for 5 min in acetone and methanol, respectively, and dried in a stream of nitrogen. A thin layer of titanium (2 nm) followed by 10 nm of gold was deposited by e-beam evaporation on these slides. We spin-coated a thin layer ($\sim 3 \mu\text{m}$) of positive photoresist (Shipley 1818) at 2000 rpm for 40 s on these gold-coated slides and heated it on a hot plate at 105 $^\circ\text{C}$ for 3.5 min. This layer of photoresist was exposed through a chrome mask, patterned with 40- μm (or 100- μm) circles spaced by 100 μm (or 120 μm), for 12 s in a Karl Suss mask aligner with a UV light source (365–405 nm) to generate circular posts of photoresist after development (Microposit 351 developer, diluted 5:1 with deionized water). The photoresist posts on the slides were heated at 150 $^\circ\text{C}$ for 30 min to melt the photoresist to form lenses. After making electrical connections to the thin gold layer with silver epoxy (SPI Supplies,

West Chester, PA), we electroplated ~ 100 nm of nickel onto the exposed gold area for ~ 2 min at a current density of 10 mA/cm^2 in a warm ($\sim 45^\circ\text{C}$) nickel sulfamate electroplating bath (Techni-Nickel "S", Technic Inc., Providence, RI). A liquid prepolymer of PDMS (mixture of prepolymer and catalyst with mass ratio 10:1) was degassed for 1 h in a desiccator under a house vacuum and spin-coated onto the microlens arrays at ~ 300 rpm for 50 s to generate a thickness of $\sim 270 \text{ }\mu\text{m}$ for the $40\text{-}\mu\text{m}$ lens arrays; heating in a 60°C oven for 3 h cured the PDMS. For the $100\text{-}\mu\text{m}$ lens arrays, we calculated the weight of the desired amount of PDMS (density $\sim 1.04 \text{ g/cm}^3$) and weighed the liquid PDMS directly on top of the lens arrays. After the liquid PDMS was let to spread across the whole surface of the lens arrays for ~ 30 min, we cured the PDMS membrane at 60°C in an oven for 3 h.

Micropattern Generation. The microlens array reduction photolithography was performed in a dark room; a dim light was used for vision. An overhead projector capable of illumination at 4000 lm (410 W/82 V, Apollo, Ronkonkoma, NY) was used as the broadband illumination source for the reduction lithography. A ground glass diffuser (1.6 mm thick, Edmund Industrial Optics, Barrington, NJ) was placed in front of the bulb, inside the housing of the projector. The desired figure was designed on CAD computer software (Macromedia Freehand 10, San Francisco, CA) in a $2 \times 2 \text{ in.}^2$ area and printed on a transparency film with a desktop printer as photomask (resolution 600 dpi). The mask was placed on the overhead projector with the designed figure at the center of the projector. Substrates for pattern formation were prepared by spinning photoresist onto Si wafers. These substrates were placed in conformal contact with the PDMS membrane covering the microlens array. The entire assembly (i.e., the lens array, PDMS membrane, and photoresist) was situated on a vertical stage ~ 50 cm above the photomask. With the lenses

situated between the light source and the imaging photoresist, white light was passed through the mask and focused by the lenses on the photoresist. The exposed photoresist was developed in a NaOH-based developer (351 developer, 5:1 diluted with deionized water). The samples were dried in a stream of nitrogen.

Liftoff of Micropatterns. The substrates for lift-off were prepared by spinning photoresist of Shipley 1805 (4000 rpm for 40 s) on Si wafers. Typical exposure times were 60–90 s, and development times were between 1 and 2 min. After development, a Cr layer (30 nm thick) was deposited by e-beam evaporation onto the samples, and the photoresist was removed by lift-off in acetone. The Cr patterns on Si were imaged by a scanning electron microscope (LEO digital scanning electron microscope, model 982).

Gray Scale Patterning. The substrates for gray scale lithography were prepared by spinning Shipley 1818 (2000 rpm for 40 s) on Si wafers. Typical exposure times were 20–45 s, and development times were fixed at 2 min. The patterned arrays in photoresist were imaged in an optical microscope (Leica Microsystems Inc., Depew, NY) and with an atomic force microscope (Digital Instruments, Santa Barbara, CA). The profile measurements of the ramp structures were done with a profilometer (Alpha-step 200, Tencor Instruments Inc., Mountain View, CA).

ACKNOWLEDGMENT

This research was supported by DARPA, MLP (N66001-98-8915), and NSF (ECS-0004030). T.W.O. thanks NIH for a post-doctoral fellowship.

Received for review March 8, 2002. Accepted April 26, 2002.

AC020151F